Polymer Bulletin
https://doi.org/10.1007/s00289-024-05477-6

ORIGINAL PAPER

Facile synthesis of interpenetrating polymeric nexus for controlled drug delivery of 5-fluorouracil (5-FU)

Maria Malook[1] · Asif Mahmood[2] · Hira Ijaz[3] · Rai Muhammad Sarfraz[4] · Muhammad Rauf Akram[4] · Bilal Haroon[1,4] · Zulcaif Ahmad[5] · Sadaf Ayub[6] · Faisal Gulzar[7]

Received: 17 January 2024 / Revised: 25 June 2024 / Accepted: 23 August 2024

Abstract

The purpose of the current research study was to formulate and evaluate a fenugreek (FG) and agarose (AG) base hydrogel exploiting pH-responsive attributes and colon targeting of 5-fluorouracil (5-FU). A novel 5-FU loaded fenugreek (FG) and agarose (AG) base hydrogel was formulated via free radical polymerization by employing N', N'methylene bisacrylamide (MBA) as a crosslinker and methacrylic acid as a monomer. The influence of substrate concentrations (FG, AG, MBA, and MAA) was studied on the swelling index, sol–gel fraction, and drug release rate (%). It was also evaluated that as the concentration of fenugreek and agarose increases, drug release increases to 94.35 ± 0.34 (%) at pH 7.4 and 13.34 ± 0.34 (%) at pH 1.2. However, an increase in MAA concentration further leads to an increase in swelling, 95.87 ± 0.23 at pH 7.4 and 14.35 ± 0.74 at pH 1.2. Moreover, MBA concentration could significantly and directly influence the swelling of hydrogels owing to the variation of crosslinking density. An increase in MBA concentration results in a significant decrease in swelling. Fourier transform infrared spectroscopy (FTIR) depicted the grafting of polymers (FG and AG) and monomers (MAA). Thermal behavior showed that the formulated nexus protects the drug and substrate from degradation. The X-ray diffraction analysis (XRD) revealed that the entrapment of the drug within the nexus mimicked its crystalline behavior. The scanning electron microscope (SEM) elucidates the porous, rough, irregular, and asymmetric nature of the nexus. Toxicity studies showed that the best-selected optimized formulated nexus (F9) is biocompatible, non-toxic, and promising for targeted delivery of 5-FU for curing colorectal cancer.

Extended author information available on the last page of the article

Published online: 06 September 2024

Graphical Abstract

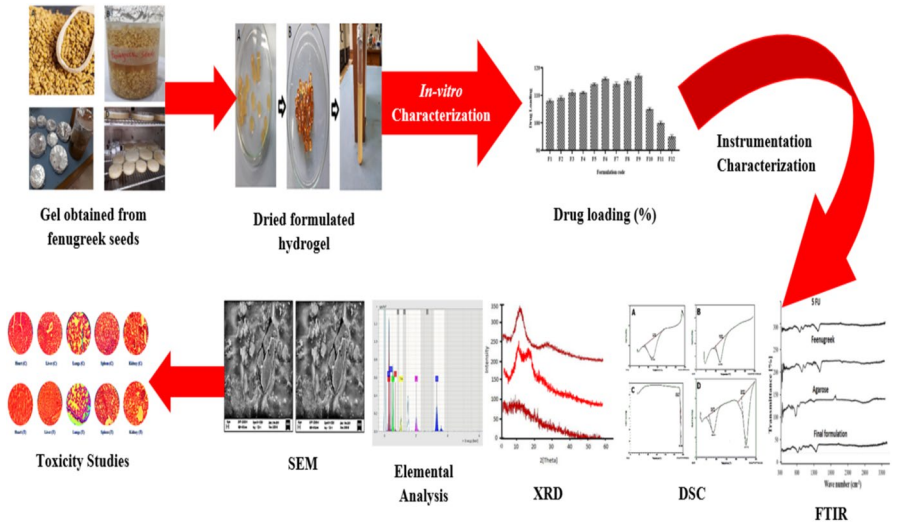

Keywords Agarose (AG) · Fenugreek (FG) · Hydrogel · 5-fluorouracil (5-FU) · Methacrylic acid (MAA)

Introduction

Among cancers, adenocarcinoma of the colon is the prevailing malignancy of the gastrointestinal tract (GIT), the third most common cancer globally, and a major cause of mortality worldwide. 5-Fluorouracil (5-FU) is an anti-neoplastic agent that belongs to the BCS class III drug and is widely prescribed in the treatment of colorectal cancer [1]. It acts by blocking the production of deoxy ribonucleotides that are essential for DNA replication, leading to cell death. However, oral delivery of 5FU is not preferred because of its variable absorption and cellular toxicity [2]. Moreover, it has a short plasma half-life of 8–20 min, poor bioavailability, and high toxicity [3]. To address these shortcomings, researchers have explored various approaches. Targeting chemotherapeutic agents aids in overcoming the limitations associated with traditional chemotherapeutic agents, like poor solubility, absorption, low volume of distribution, and toxicity [4]. Moreover, conventional chemotherapeutic agents do not reach the target site in effective concentration, and an increase in drug dose leads to enormous toxicity [5]. Various other therapeutic and surgical approaches have been reported in the literature to treat colorectal cancer, but these approaches have limitations [6]. pH-responsive nexus is one of the promising approaches to overcome these limitations. However, many polymeric materials of natural origin have been extensively employed for formulating these pH-responsive nexuses, like xanthan gum, starch, alginate,

etc. The structure and composition of natural polymers amalgamate their biological as well as physical attributes, which play a vital role in new product development [7]. The activity of natural polymers is attributed to their composition, which includes carbohydrate backbone and pendent groups. Furthermore, they are biodegradable, biocompatible, and non-allergic. Among natural polymers, agar and fenugreek have been employed for biomedical purposes and are the most studied polysaccharides.

Trigonella foenum-graceum, commonly called Fenugreek, is a biopolymer belonging to the family Leguminosae. Fenugreek gum is extracted from fenugreek seeds, which consist of D-galactopyranosyl and D-mannan groups [7]. It contains different useful substances (with variable applications) like mucilage (28%) and gums (23%), and is a rich source of galactomannan with fascinating diverse attributes like thickening, gelling, emulsifying, and suspending agents [8].

Agar is a hydrophilic, biodegradable polysaccharide with an enormous number of hydroxyl moiety that forms intermolecular and intramolecular H-bonds. It is a linear polysaccharide with an idealized structure consisting of repeating agarobiose and alternating β-D-galactopyranosyl and 3, 6-anhydro-α-L-galactopyranosyl units obtained from the cell walls of red algae and seaweed. Moreover, the backbone is masked by substituent moieties like methyl ether and sulfate ether that upgrade its gelling attributes [8]. A literature survey supports that agar is biodegradable, non-toxic, and offers excellent gelling properties. Agarose-based hydrogels have been prepared in the literature for controlled delivery of different therapeutic agents [9].

Methacrylic acid (MAA) is a polyanionic monomer with -COOH moiety and exhibits low swelling at a pH lower than pKa (4.26) [8]. As hydrogel enters the GIT, pH gradually increases (from the stomach (1.2) to the small intestine (7.4)), hydrogel swelling increases, which is related to electrostatic repulsion within ionized pendent moieties, and stretching of the coiled network occurs, which results in drug release [9, 10]. Hydrogel formation is attributed to the polymerization of MAA with a bifunctional crosslinker, N, N-methylene bis-acrylamide (MBA), and the initiator ammonium persulfate (APS) [11–13]. The structure of the polymer-monomer crosslinker is shown in Fig. 1.

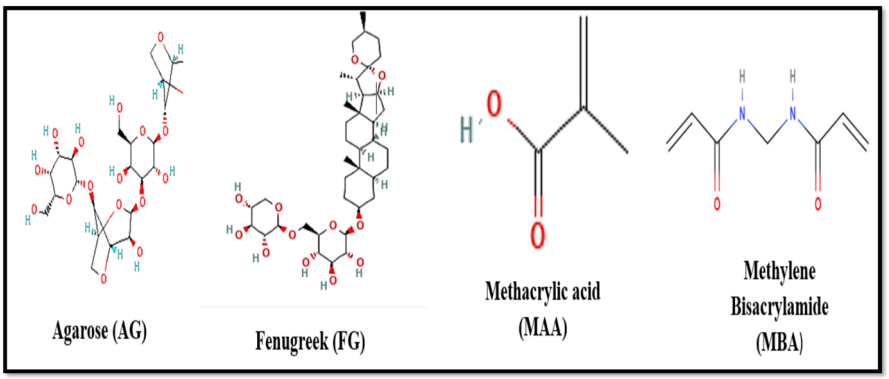

Fig. 1 Different Polymers, monomer and crosslinkers

A literature survey supports the fact the fact that, up until now, no research work has been published on environmentally friendly and economical 5-FU-loaded FG/AG-co-MAA-based hydrogel. So the current research study focuses on developing novel, pH-sensitive, bio-compatible FG/AG-co-MAA-based hydrogels for targeted delivery of 5-FU for treating adenocarcinoma of the colon.

Material and methods

Materials

5-FU, methacrylic acid (MAA), ammonium per sulfate (APS), and N, N, methylene bis-acrylamide (MBA) were purchased from Sigma-Aldrich. Potassium dihydrogen phosphate ($K_2H_2PO_4$), sodium hydroxide (NaOH), hydrochloric acid (HCl), n-hexane, and ethanol were procured from CCL Pharmaceuticals, Lahore, Pakistan. Fenugreek seeds were obtained from the local market in Lahore. All chemicals were of analytical grade.

Methods

Extraction of fenugreek polymer

Fenugreek seeds were weighed accurately on an electronic weighing balance. 100 g of weighed seeds were taken in a 1000 mL beaker. Then these dipped seeds were placed in a microwave oven for at least 3 days at 40 °C. These seeds were allowed to swell, and the gel was extracted by using a muslin cloth. The extracted gel was washed with n-hexane for 15–20 min. Gel content was precipitated down, n-hexane was decanted, and pure gel was obtained. Gel was transferred into these Petri dishes and placed in a microwave oven at 40–45 °C for 2 weeks until properly dried. This dried gel was removed from all petri dishes by using a spatula and transferred into a pestle and motor, followed by grinding to obtain a fine powder (Fig. 2) [14].

Method of preparation of hydrogel

Hydrogel was prepared by the free radical polymerization technique. All the ingredients were properly weighed. Agarose was dissolved in 20 mL of distilled water on an electronic hot plate magnetic stirrer at 70 °C for at least 2 h until a uniform solution was formed. The beaker was removed from the hot plate stirrer to cool the mixture, and it was covered with aluminum foil (Polymer solution I). In another beaker containing fenugreek polymer, 20 mL of distilled water was added and subjected to a stirrer for 10 min until the formation of a clear solution. The beaker was removed and covered with aluminum foil (polymer solution

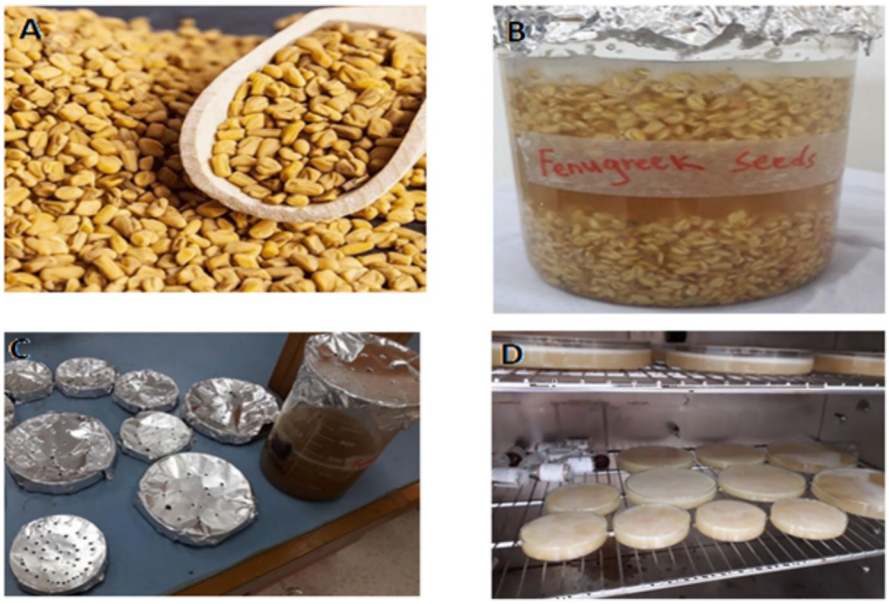

Fig. 2 Fenugreek seeds (**A**), Swelled fenugreek seeds (**B**), Gel obtained from fenugreek seeds (**C**), Drying of fenugreek gel (**D**)

II). Fenugreek solution was added dropwise into agarose solution on a hot plate magnetic stirrer, followed by the addition of APS solution; active sites were generated on polymer sites. After that, MAA was added to the above polymeric mixture to saturate active sites. Finally, MBA was added to initiate cross-linking. The test tubes were taken, properly washed, and dried. The above solution was added to these test tubes and sonicated for 3 min so that any bubbles present in the solution could be removed. Then this sonicated solution was added to centrifugation tubes and subjected to centrifugation for 5 min at 450 rpm. The centrifuged solution was placed in test tubes again; these tubes were covered with aluminum foil and placed in a water bath at 65 °C for 24 h. Upon the formation of hydrogels, test tubes were transferred into plastic bags individually, broken down by the wooden back of the test tube holder. The obtained hydrogels were washed to remove any surface glass. These hydrogels were transferred into 250 mL beakers and washed with distilled water and ethanol (50:50). Washed hydrogels were transferred into petri dishes and dried in a hot air oven until they reached a constant weight. Dried hydrogels were kept in a desiccator for further use [15, 16]. The presumptive diagram is shown in Fig. 3. Formulated hydrogel is shown in Fig. 4.

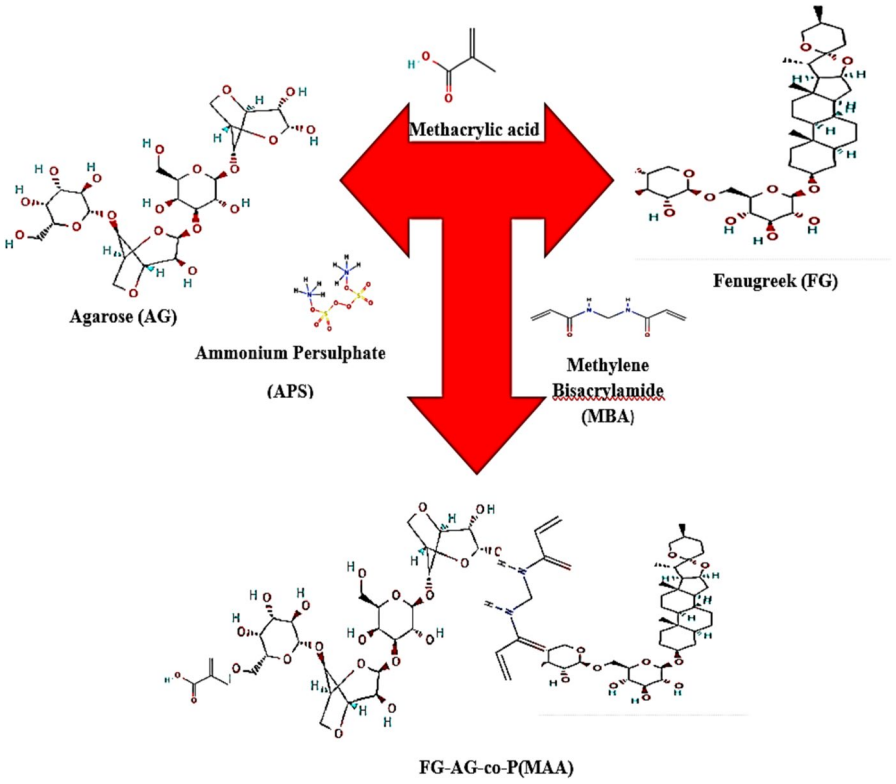

Fig. 3 Presumptive Diagram

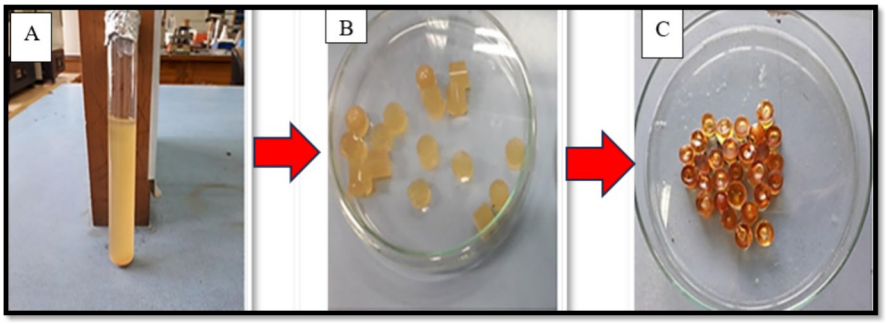

Fig. 4 Gel in glass vial (**A**), discs (**B**), and dried discs (**C**)

Physical examination

All the developed formulations (F1-F12) were physically examined for appearance, stickiness, fragility and color, etc.

Swelling studies

The dried hydrogel discs of each formulation were accurately weighed and immersed into solutions of pH 1.2 and 7.4 until they were completely swelled and there was no further increase in weight. Note the weight of each dipped formulation after a half hour: 1, 1.5, 2, 3, 4, 5, 6, 8, 10, 12, 14, 16, 18, 24, 30, and 36 h, respectively. The swelling index was determined by using this formula [8].

$$Swelling\ index = \frac{W_t - W_o}{W_o} x100$$

where, W_o = weight of dried hydrogel disc and W_t = weight of wet or swelled hydrogel disc at time (t) (28).

On–off switching

pH responsiveness was evaluated by on–off switching behavior. Formulation F9 was allowed to swell at pH 7.4 after sometimes hydrogel disks were subjected to pH 1.2, which undergoes deswelling. Such on–off switching patterns were observed for up to 3–4 cycles.

Sol–gel fraction (%)

To determine the number of reactants polymerized in the preparation of hydrogels, the sol–gel fraction was determined. Prepared dried hydrogel discs were subjected to soxhlet extraction for 4 h at 100 °C. Unreactive contents were removed, and these gels were dried in hot air at 45 °C until a constant weight was achieved. The Sol–gel fraction was calculated by following the equation [9].

$$Sol\ fraction(\%) = \frac{W_a - W_o}{W_a} x100$$

$$Gel\ fraction = 100 - Sol - fraction$$

where, W_a = weight of dried gel after extraction and W_o = weight of dried gel before extraction [17].

Drug loading (%)

Drug loading in the hydrogel was done by the diffusion method. A 1% solution was prepared by dissolving 1 g of 5-FU in 100 mL of phosphate buffer of pH 7.4 along with continuous stirring. The dried disc hydrogels were allowed to be immersed in a buffer solution for up to 48 h so that complete loading of the drug had been done. Drug-loaded hydrogel discs were removed from the buffer solution and washed with distilled water for 2 min to remove the adhered drug. These

washed discs were placed in Petri dishes and transferred to the oven for complete drying at 40 °C for 5–6 days so that they could achieve a constant weight [3].

Mechanical strength

This test was performed to determine the tensile strength of developed hydrogels. 10 kN loaded chamber and TIRA software was attached with tensile tester. Optimized hydrogel formulations were placed in between static and mobile jaws of the tester. Now this machine was operated at 50–55 mm per min. Stress was developed (force per unit area) and strain that was any change in its length was compared with its initial length and final length of hydrogels. Formula was used to determined difference [10].

$$\sigma = \frac{F}{\pi r^2}$$

where, force that was exerted on hydrogels r = radius of sample.

$$\varepsilon = l - lo / lo\varepsilon = \text{strain}$$

lo = initial length of hydrogels l = final length of hydrogels [18].

FTIR spectroscopic evaluation

Fourier transform infrared spectroscopy (FTIR) (Bruker, Germany) analysis was carried out on 5-FU, agarose, fenugreek, MBA, and an optimized hydrogel formulation. All the samples were crushed with a pestle and mortar. Samples were examined one by one at a scanning range of 4000–600 cm^{-1} by using the ATR (attenuated total reflectance) technique [8, 9].

Thermal analysis

Differential scanning calorimetry (DSC)

Differential scanning calorimetry (DSC) (Perkin Elmer) was the technique employed for analysis of the thermal behavior of individual ingredients and optimized formulation. Each dried sample was accurately weighed and crushed in a mortar and pestle. It was placed in an aluminum DSC pan in a hermetically sealed condition. Measurements were carried out in the range of 0–400 °C in an oven with a heating rate of 10 °C/min [15].

Thermogravimetric analysis (TGA analysis)

TGA was performed on a thermogravimetric analyzer (Perkin Elmer). TGA studies were performed to identify physical and chemical changes in substrate and formulation with rising temperatures. All the samples were placed in a sample holder and analyzed under nitrogen purge, along with heating at 10–20 °C/min from 20 to 500 °C. Mass loss with respect to temperature was determined [16].

X-ray diffractometer (XRD) studies

Powder forms of dried hydrogels, pure drugs, and polymers were taken. An XRD diffractogram was recorded via an x-ray diffractometer (Thermo Fisher Scientific). For the scanning level on the glass surface, a copper-ka source was used to analyze samples [9].

SEM (scanning-electron microscopy)

To analyze the structural morphology of the dried hydrogel formulation properly, SEM (Thermo Fisher Scientific) was employed. Hydrogel was covered with a double layer of aluminum-gold sputter under an argon atmosphere. Scanning of superficial morphology was done on the dried hydrogel formulation [9, 10].

Energy-dispersive spectroscopy (EDX)

EDX studies were performed to identify the elemental composition of hydrogel formulations. The elements consist of atoms and emit x-rays, along with an accurate amount of energy transfer. Energies that were emitted from x-rays were used to identify the element. An energy-dispersive x-ray was used to analyze the hydrogel to determine the presence of carbon, nitrogen, oxygen, and sodium. This test was also performed to identify the presence of the drug in the prepared hydrogel [19].

In-vitro studies of 5-fluorouracil

Release studies were done by using a dissolution apparatus (USP dissolution apparatus Type II) (Thermo Fisher Scientific). pH responsiveness and release of 5-FU from Fenugreek-Agarose-based hydrogels were calculated or determined at pH 1.2 and 7.4. Dried-loaded hydrogel discs were dipped into the buffer at pH 1.2 and 7.4 in the dissolution apparatus for 24 h at 37 C at 50 rpm resolution speed. 5 ml of samples were withdrawn from the solution after every 1 to 2 h. Freshly prepared buffer was added to the dissolution media to maintain the pH level. After 24 h, discs were removed from the solution media, and samples were analyzed on a UV spectrophotometer [15].

Analysis of the results

Model-dependent approach

Kinetic analysis

Data obtained from the in-vitro drug release mechanism was processed using different kinetic models, like the zero-order, first-order, Higuchi model, and Korsmeyer-Peppas model. The best-fit model was determined by using DD solver software. To find out the best model, correlation coefficient (R^2) values were used [16].

$$\text{Zero order} = Q_t = Q_o - K_o$$

$$\text{First order} = LnQ_t = LnQ_o - K_1 t$$

$$\text{Korsmeyer} - \text{Peppas model} = Q_t = Q_o - K_o$$

$$\text{Higuchi model} = Q_t = Q_o - K_o \text{ [33]}$$

Q_o = Initial amount of drug in hydrogel.
Qt = Amount of drug after time 't'.
K_o, K_1 and K_H are rate constants of the respective executed kinetic model.
Here, M_t/M_∞ is the portion of drug released at time t, K is drug release rate constant and *"n"* is release exponent.

Model-independent approach

Statistical analysis Statistical analysis was performed for raw data of all parameters using ANOVA (one-way ANOVA) on the DD Solver add-in Excel program by taking a significance value less than 0.05. It is employed to assess the comparability between drug dissolution profiles [9].

Similarity and difference factors The similarity index (*f2*) and difference (*f1*) index were determined by using the below equations (DD solver adds in Microsoft Excel program) [9]. The difference factor (*f1*) helps in calculating the percent difference in two curves per unit of time "t" and measures the relative error in the two curves.

$$f1 = \{[\sum_{t=1}^{n} Rt - Tt/[\sum_{t=1}^{n} Rt]\} \times 100$$

The similarity factor ($f2$) is a logarithmic reciprocal square root transformation of the sum of squared error and is a measurement of the similarity in the percentage dissolution between the two curves.

$$f2 = 50 \times \log\{1 + (1/n)St = \ln(Rt - Tt)2{-}0.5 \times 100$$

Accelerated Stability Studies Stability studies were conducted by keeping the optimized formulation within the stability chamber to ensure effectiveness throughout the product's shelf life. The International Council for Harmonization (Anex-10 ICH) guidelines were followed to conduct accelerated stability studies under accelerated conditions of humidity (75% RH) and temperature (40.2 ± 2 °C) for up to 6 months [20]. Hydrogels were evaluated physically (color, swelling, drug contents, and percentage of drug release).

Toxicity studies To perform this study on animals, approval was obtained from the Institutional Research Ethical Committee (IREC-2020–44) at the University of Lahore. Six healthy adult male albino rabbits were used. They were placed in the animal house at the university. These rabbits weighed about 2–2.5 kg. Rabbits were housed in safe and ventilated cages. According to the Organization for Economic Co-operation and Development (OECD), a tolerated dose was given to rabbits. Rabbits were divided into 2 groups: one was a controlled group (dose was not given), and another was a tested group (dose was given). Before giving the dose, rabbits were kept fasting for 24 h. Animals were examined for general conditions like water and food intake, any increase or decrease in body weight, their response to stimuli, strength of grip, corneal reflex, hyperactivity, etc. Blood samples were taken 7 days after giving the dose. The sample was taken with a 5-mL syringe from the jugular vein of the ear. On the 14th day, rabbits were sacrificed, and vital organs were taken for histopathological examination. Ketamine 1.4 mL and xylazine 0.6 mL injections were used as anesthesia; they were injected into rabbits, and after that, rabbits were sacrificed, and vital organs (kidney, liver, lungs, spleen, heart, brain, and small intestine) were removed. They were cleaned and preserved in an airtight container with a 10% formalin solution in them. Slides were prepared for observing these organs under an electron or optical microscope [19].

Results and discussion

Fenugreek-agarose-based hydrogels were formulated via the free radical polymerization technique. For chemical cross-linking between reactants, a chemical reaction was initiated by using N, N-methylene bisacrylamide (MBA) as a cross-linker and ammonium persulfate (APS) as the initiator. Four sets of formulations (F1–F12) were formulated as shown in Table 1.

Table 1 Composition of hydrogel

Formulation	Fenugreek (FG) (g/100gm of hydrogel)	Agarose (g/100gm of hydrogel)	Methacrylic acid (MAA) (g/100gm of hydrogel)	MBA (g/100gm of hydrogel)	APS (g/100gm of hydrogel)
F1	0.3	0.5	10	0.13	0.13
F2	0.6	0.5	10	0.13	0.13
F3	0.9	0.5	10	0.13	0.13
F4	0.9	1	15	0.15	0.15
F5	0.9	1.5	15	0.25	0.15
F6	0.9	2	15	0.25	0.15
F7	0.3	1	20	0.25	0.13
F8	0.3	1	25	0.25	0.13
F9	0.3	1	30	0.25	0.13
F10	0.3	1	20	0.25	0.15
F11	0.3	1	20	0.50	0.15
F12	0.3	1	20	0.75	0.15

Physical appearance

All formulations were examined physically and exhibited a yellow color due to the presence of fenugreek, smooth, elastic, jelly-like consistency, and soft texture. The formulation in which the agarose concentration was significant has a white color, is translucid, jelly-like, and slightly hard in texture, as shown in Fig. 4.

Equilibrium swelling ratio

The absorption capacity of hydrogel (swelling behavior) directly influences drug loading and release. The swelling ratio of the formulated nexus was observed in different testing media (phosphate buffer) of variable pH, i.e., 1.2 and 7.4, at 37 °C, as shown in Fig. 5. Hydrogel undergoes swelling between pH 1.2 and 7.4, and the swelling rate varies over the range of pH. The formulated nexus depicts significant swelling at pH 7.4 as compared to pH 1.2. Swelling is attributed to the protonation and deprotonation of -COOH moiety of the monomer. During protonation, -COOH moiety undergoes conjugation with counterions via H-bonding, as a result of which the charge density of the COOH group decreases and results in low swelling at pH 1.2. Moreover, at pH 7.4, the charge density of the COOH group increases, and the arboxylic acid group ionizes at pH 7.4. The carboxylic acid group ionizes to a carboxylate ion (COO-) and electrostatic repulsion results in macromolecular expansion, thereby decreasing hydrogen bonding and consequently resulting in an increase in swelling. Moreover, the hydroxyl moiety was ionized via water and resulted in augmented swelling. Significantly higher values were also reported by Ijaz et al. (2017 [11] and Azam et al. (2017) [21].

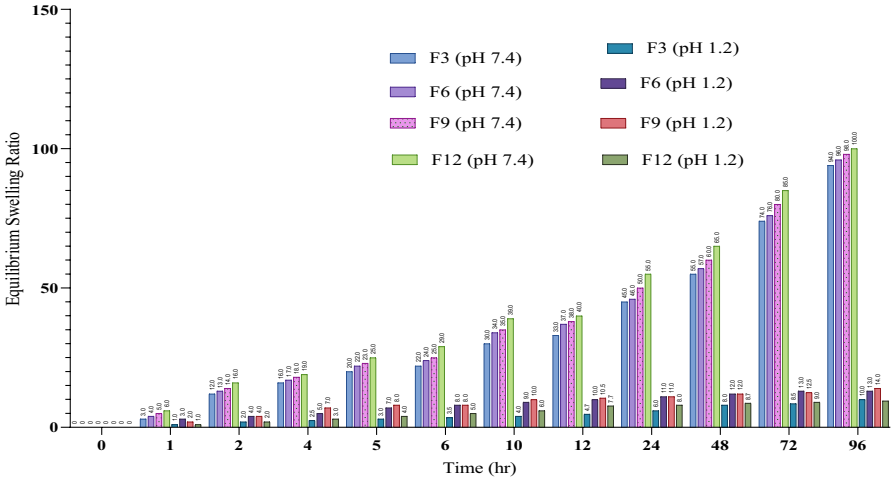

Fig. 5 ESR of formulation F3, F6, F9 and F12

Hydrogel was formulated by varying concentrations of polymer/monomer and crosslinkers to investigate the influence of substrate on swelling ratio across multiple media. For swelling studies, formulations (F3, F6, F9, and F12) with significant concentrations of polymers, monomers, and crosslinkers were selected, and equilibrium swelling studies were conducted at pH 1.2 and 7.4 (Fig. 5). Formulation F3 containing 0.9 g of fenugreek showed an ESR of 94.74 ± 0.87 in pH 7.4 and 10.74 ± 0.34 in pH 1.2. Batool et al. (2021 prepared a fenugreek-based intelligent polymeric nexus and showed similar facts [14]. Formulation F6, in which agarose content was increased to 2 g, depicted a swelling ratio of 96.35 ± 0.34 in pH 7.4 and 13.34 ± 0.34 in pH 1.2. Hu et al. (2021 fabricated flexible pH-sensitive agarose and succinoglycan hydrogels for controlled drug release and reported a similar fact [22]. The decreased ESR of F3 as compared to F6 is attributed to the fact that fenugreek-base hydrogel maintains real geometry in an aqueous environment due to its gummy nature. Moreover, the remarkable increment in swelling ratio and polymer chain expansion is attributed to the electrostatic force of repulsion, which may be due to a negatively charged polymeric moiety (agarose and fenugreek). However, formulation F9 with a significant concentration of monomer (30 g) depicted a remarkable increase in swelling as compared to formulations F3 and F6. F9 showed an ESR of 98.87 ± 0.23 at pH 7.4 and 9.35 ± 0.74 at pH 1.2. In formulation, F9 methacrylic acid (MAA) content was significant and has resulted in a significant increment in equilibrium swelling, which is attributed to electrostatic repulsion between ionic species and disruption of hydrogen bonding within polymeric chains, which leads to the breaking of hydrogen bonding interactions. Due to electrostatic repulsion, the osmotic pressure inside the hydrogel network was increased, resulting in a higher uptake of hydrogen ions and an uptake of swelling media, resulting in higher swelling in the basic pH. Similar facts were observed by Ijaz et al. (2022) while working on a CS-co-P(AA)-based

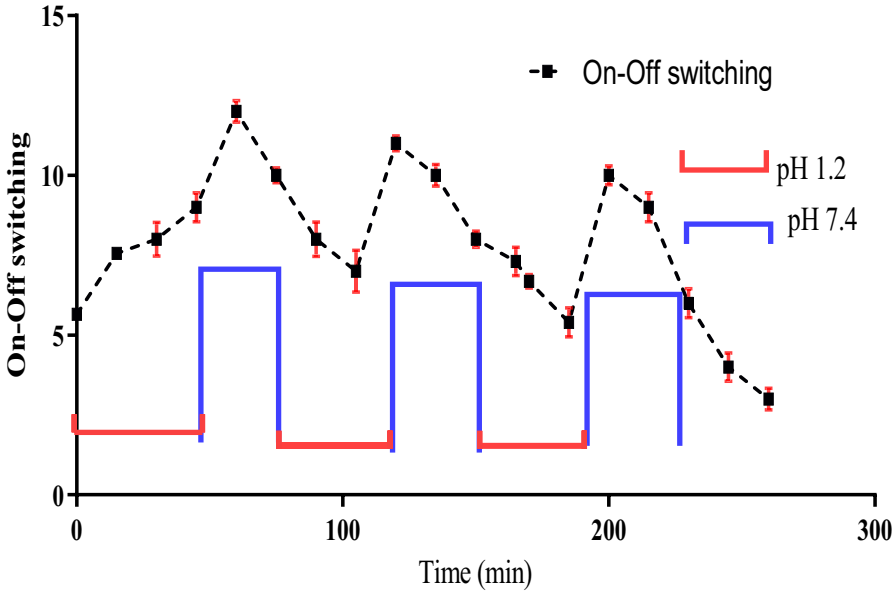

Fig. 6 on–off switching of formulation F9

perindopril erbumine loading nexus for targeted drug delivery [8]. Formulation F12, containing 0.75 g MBA, showed reduced swelling, which is attributed to increasing cross-linking density; the hydrogel swelling ratio was decreased, and a number of available hydrophilic groups were occupied. Azam et al. (2019 formulated perindopril-erbumine-loaded AX-co-P(MAA) nexus and postulated the fact that an increase in crosslinker concentration led to a decrease in swelling [21].

On–off switching and pH reversibility

The optimized formulation exhibited reversible hydration (swelling) and dehydration (shrinking) accompanied by volumetric transitions in response to external media. Figure 6 shows the pulsatile/reversible on–off switching behavior of hydrogel (F9), which depicts controlled drug delivery from the nexus. pH sensitivity is attributed to the pendent group, which accepts and donates H-ions. With the increase in pH, swelling increased remarkably. Moreover, a partially hydrolyzed nexus contains a carboxylate moiety, which either accepts or releases H + ions in response to the surrounding environment. At pH 7.4, ionization of the carboxylate group occurs, and electrostatic repulsive forces between charged sites result in hydrogel swelling. However, at pH 1.2, protonation of carboxylate ions results in the elimination of anionic-anionic repulsion; consequently, swelling is decreased, and a remarkable decrease in equilibrium swelling is observed (gel collapsing). Moreover, hydrogel recovery in the swelling phase

is a slower process than in the de-swelling phase. Initially, hydrogel water content increases in the first several minutes. Afterwards, at pH 1.2, the swelling process undergoes deceleration. After 3–4 cycles, hydrogels remained intact and undamaged, which demonstrates the good mechanical strength of hydrogels. Reversible swelling de-swelling demonstrated excellent pH sensitivity and potential application as a pH-responsive biomaterial. Ijaz et al. (2022 reported a similar fact [14].

Sol–gel fraction (%)

Hydrogels are prepared via a polymerization reaction. When some components of the substrate do not undergo polymerization reactions, this is known as the "sol fraction" and is attributed to the high quantity of uncrosslinked formulation constituents, whereas the crosslinked fraction is termed the "gel fraction." Moreover, sol fraction resulted when a sufficient quantity of substrates was involved in polymerization, and they remained uncrosslinked due to insufficient reactive sites in the polymerization reaction. Crosslinked and uncrosslinked proportions of the substrate can be evaluated via sol–gel analysis. The increase in gel fraction is directly related to the concentration of polymer, monomer, and crosslinker. As polymer and monomer concentrations increase, the number of side chains implicated in crosslinking also increases, and as crosslink concentrations increase, crosslink density also increases. Hence, the ratio of uncrosslinked reactants will be lower. We performed the Sol–gel fraction on all hydrogel formulations (F1–F12) to investigate the impact of polymers, monomers, and cross-linkers on the gel fraction. Dried hydrogel discs of each formulation were weighed and broken down into tiny pieces, then dipped in 250 mL of distilled water for at least 4 h at 100 °C. The sol fraction revealed the amount of unreactive monomer and cross-linker. The formulation, i.e., (F1-F3), containing a significant concentration of fenugreek, depicted a remarkable gel fraction (83.55–89.53%), as shown in Fig. 7. The maximum gel fraction was seen in formulation F3, i.e., 89.53%, and the sol fraction was 11.58%. While the increase in agarose concentration in formulation F4-F6 increased, the gel fraction (%) increased

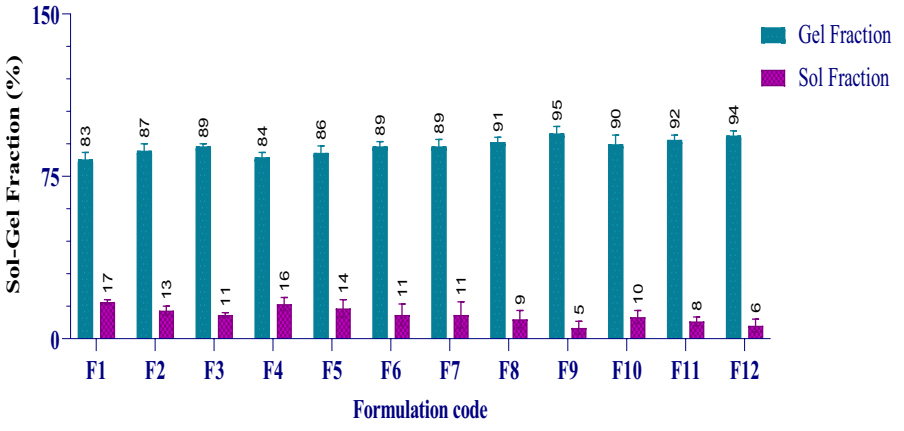

Fig. 7 Sol gel fraction of formulation F1 to F12

incrementally (84.33–89.93%). The literature review supports the fact that as polymer concentration increases, polymeric coils couple, and this is accompanied by the coils surrounding the coiled nexus, resulting in the formation of interpenetrating, overlapping entanglements between the coils [17]. Formulation F9 containing a significant concentration of MAA showed a gel fraction of $95.34 \pm 0.34\%$ and a sol fraction of $5.73 \pm 0.24\%$, which is attributed to the fact that as monomer (MAA) concentration increases, it leads to an increase in the availability of space, which increases swelling. Rana et al. (2022) synthesized cellulose acetate-based grafted gel and observed an increase in gel fraction with an increase in monomer concentration [23]. In formulations F10–F12, crosslinker (MBA) was increased, resulting in an increase in gel fraction, which is attributed to significant crosslinked density and the availability of more substrate, which increases gel fraction. Rahmani & Shojaei (2022) developed a tough terpolymer hydrogel with outstanding swelling ability using hydrophobic association cross-linking and observed the analog effect of MBA on gel fraction [24].

Drug loading

5-FU (fluorouracil) was loaded in all prepared hydrogel formulations (F1–F12) via swelling and diffusion-controlled methods. Drug loading in hydrogels depends on the pore size of the hydrogel. The extent of loading (%) of 5-FU was observed by changing the concentrations of fenugreek (F1-F3), agarose (F4-F6), MAA (F7-F9), and MBA (F10-F12), respectively. Drug loading follows the same pattern as that of ESR. 5-FU loading (%) was increased from 108 to 111% by increasing the concentration of fenugreek, as shown in Fig. 8. This increase in 5-FU loading was due to a rise in viscosity with an increment in fenugreek contents. Moreover, fenugreek has a hydrophilic nature, and developed hydrogels have resisted 5-FU leakage. In addition, as fenugreek contents rise, the availability of anionic sites in the form of hydroxyl ions increases, offering higher crosslinking and exposure to 5-FU. The agarose base formulation showed a similar pattern, and drug loading increased from 111 to 116%. However, formulations F7 to F9 containing 20 to 30 g of MAA showed drug loadings of 114 to 117%. The highest drug loading was observed in formulation F9, which is attributed to carboxylic acid group deprotonation from the monomer (MAA) and -OH moiety of fenugreek and agarose, which results in the generation of negatively charged moiety. Moreover, its hydrophilic nature, due to the increased absorbed water content of the polymeric network, contributes to the remarkable drug loading. Du et al. (2022) developed temperature- and pH-responsive carmofur-loaded nanogels and reported a similar finding [25].

Tensile strength

Mechanical strength was checked to evaluate the toughness and stiffness of the formulation. This test was performed to find out the maximum force at which

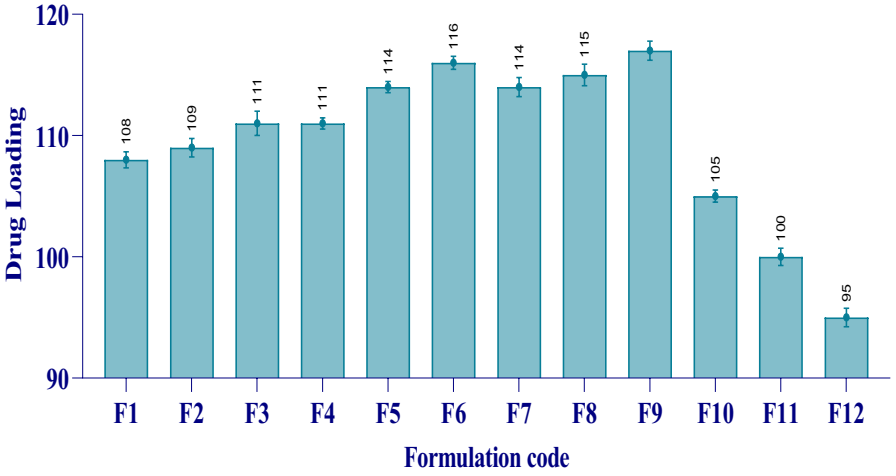

Fig. 8 Drug loading of drug loaded hydrogels (F1-F12)

Table 2 Tensile strength of Formulation F6, F9 and F12

Formulation codes	Tensile strength (N/mm^2)	Load at break (N)	Total elongation at maximum force %	Youngs modulus (N/mm^2)	Comments
F6	31.82	3.72	17.162	241.32	Breaked
F9 (Best Formulation)	43.617	4.712	26.324	364.74	Breaked
F12	49.111	4.5174	27.981	487.12	Breaked

formulated hydrogels undergo cracking. It was performed on a UTM (UTM) Universal Testing Machine). The three best 5-FU-loaded formulations (F6, F9, and F12) were selected, on which this test was performed. Table 2 and Fig. 9 showed mechanical attributes such as tensile strength, load on break, and total elongation, which are critical indicators when designing a drug delivery system. As MAA concentration increases, the gel's mechanical strength decreases. The optimized formulation F9 demonstrated a tensile strength of 43.617 N/mm2, a load at break of 4.712 N, and a total elongation of 26.32% (at maximum force). Hydrogel swelling has an impact on drug loading and release. Moreover, the optimized formulation should have sufficient mechanical strength so that the nexus retains its integrity after significant swelling and drug release. Furthermore, too high crosslink density results in a mechanically strong hydrogel, which hinders swelling as well as drug loading. The significant crosslinker concentration in the F12 formulation led to the maximum force required to break the hydrogel, as an increase in crosslink density decreases permeation. Tang et al. (2017) investigated the influence of graphene oxide/polymer base nanocomposites and discovered that stiffness and hardness increase with an

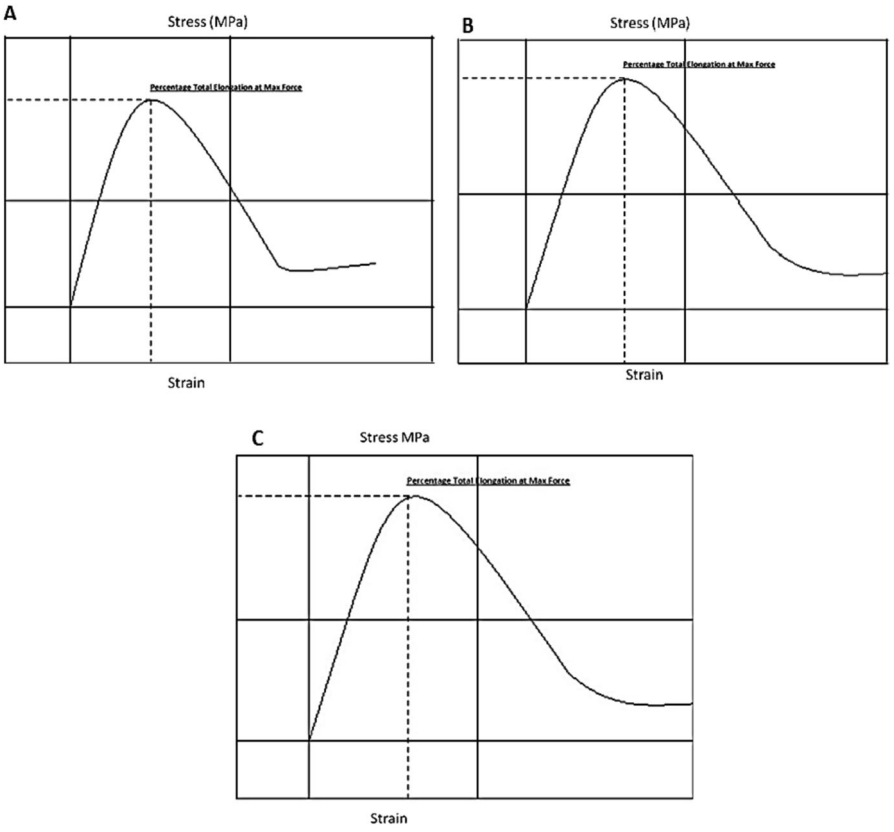

Fig. 9 Tensile strength of formulation F6 (**A**), F9 (**B**) and F12 (**C**)

increase in MBA concentration [26]. Preferably, hydrogels for drug delivery should be critically evaluated for desired attributes by varying substrate ratios and evaluating their influence on swelling, drug loading, and release.

Fourier-transform infrared spectroscopy (FTIR) evaluation

FTIR was carried out on the drug (5-FU), fenugreek (FG), agarose (AG), and formulated hydrogel (FG-AG-co-PMAA). The FTIR spectrum of 5-FU revealed a band between 3250 and 3300 cm^{-1}, attributed to NH stretching vibrations. Peaks within the range of 2791.12–3200 cm^{-1} were confined to N–H stretching vibration. The C = O stretching behavior was associated with the peaks at 1700 and 1635 cm^{-1}. Bending and stretching movements of the C-N bond were noticed at 1504 cm^{-1} and 1427 cm^{-1}, respectively. Typical peaks of 5-FU were evident at wavenumbers, i.e., 2991.11 cm^{-1}, 1707 cm^{-1}, and 1336 cm^{-1}. Abdullah and his coworkers observed the same phenomenon while formulating PVA-based 5-FU-loaded hydrogels for colon

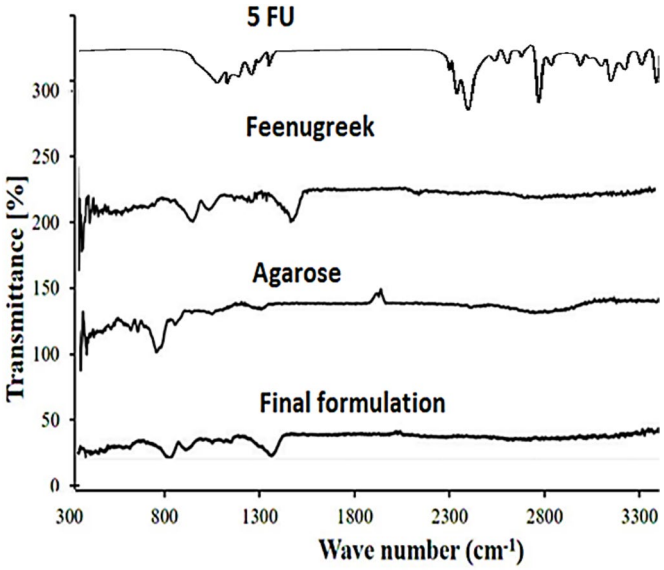

Fig. 10 FTIR spectra of drug, polymers and formulation

targeting [27]. The FTIR spectrum of fenugreek was recorded to find functional groups within the sample. The N–H stretching vibrations in fenugreek husk exhibited a characteristic absorption band at 3365 cm^{-1}. The band at 1542 cm^{-1} indicates C = O stretching vibration. These results align with El-Bahy's research from 2005, which focused on FTIR and Raman spectroscopy of fenugreek polysaccharide [28]. The agarose FTIR depicted stretching vibrations at 1190–700 cm^{-1}, which were attributed to the presence of C–O–C and COOH moiety. However, peaks at 900 cm^{-1} and 870 cm^{-1} regions were due to the presence of D-galactopyranose and β-D-mannopyranose units, respectively. Peaks within 1710–1600 cm^{-1} confirmed the presence of aldehydes, esters, ketones, and carboxylic acids. These peaks were also consistent with other research studies carried out by other researchers [14]. The FTIR spectrum of developed formulations was also recorded, and it was noticed that the FTIR spectrum of formulations showed new peaks, overlapped peaks, and the disappearance of a few peaks. Therefore, the newly grafted nexus showed a minor difference as compared to individual ingredients, which is indicative of efficient crosslinking as well as the entrapment of drugs within the nexus, as shown in Fig. 10.

differential scanning calorimetry (DSC)

DSC was performed to analyze the melting points, phase, and glass transition of all substrates. The melting point of pure, untreated polymer agarose was 81.60 °C. The initial short endothermic peak at 55 °C was due to the loss of moisture, followed by a wide endothermic band seen between 81.60 °C and 125.57 °C, which

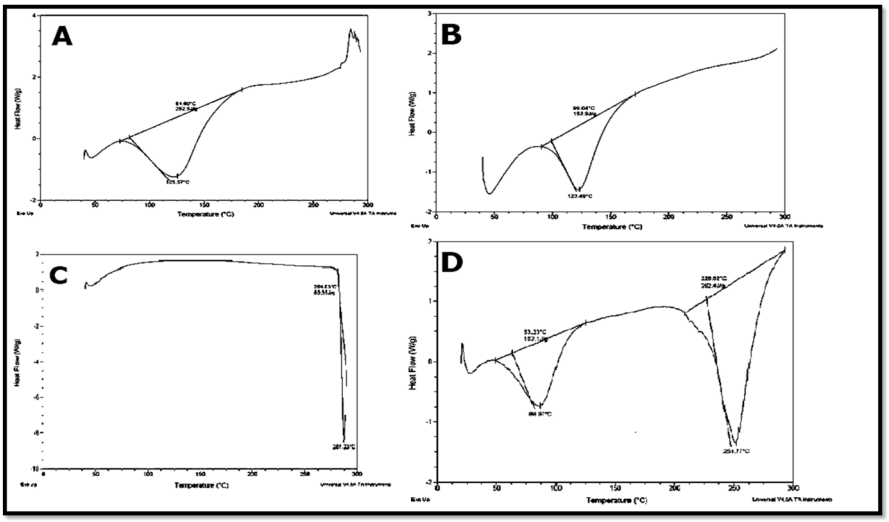

Fig. 11 DSC thermograms of Agarose (**A**), Fenugreek (**B**), 5-FU (**C**) and Final formulation (**D**)

corresponds to the melting point range of agarose. Complete burning was observed as an exothermic peak appeared at a temperature of 300 oC. H-bonding is accountable for the transition between the H + of water and the OH- moiety of polymers. Rotjanasuworapong et al. (2020) prepared biodegradable and biocompatible agarose-based hydrogels using ibuprofen as a model drug and showed that degradation of polymers occurs at 30–240 °C. DSC of fenugreek showed an initial short endothermic peak at 55 oC due to the loss of moisture, followed by a wide endothermic band seen at 99.04 oC–123.49 °C. Our results are in line with previous research studies [29]. Similar peaks were reported by Batool et al., 2021 [14]. An initial short endothermic peak of 5-FU appeared at 55 °C, attributed to the moisture loss, followed by a wide endothermic band at 284.03 °C–287.23 °C. Corresponding to the melting point range of 5-FU, complete burning was observed as an exothermic peak appeared near 300 °C. Pal et al. (2018) observe similar peaks while formulating a 5-FU-loaded sesbania gum-based hydrogel [30]. The formulated nexus showed a peak at high temperatures, which showed the formulated nexus remained stable at high temperatures. In other words, the formulated nexus protects the drug from degradation, thereby retaining its stability. All thermograms are shown in Fig. 11.

PXRD (powder X-ray diffraction) studies

XRD was conducted for all components and the fabricated hydrogel. The XRD diffractogram of 5-FU depicted sharp and evident peaks at different angles, i.e., 16.15°, 17.55°, 18.25°, 21.23°, 22.55°, 24.66°, 28.75°, 31.21°, 32.45°, 34.15°, and 37.55°. These peaks endorse the crystalline nature of pure 5-FU, as shown in Fig. 12. Similar results were reported previously while formulating a pH-responsive nexus for controlled delivery of cytarabine [14]. XRD studies of fenugreek gum were

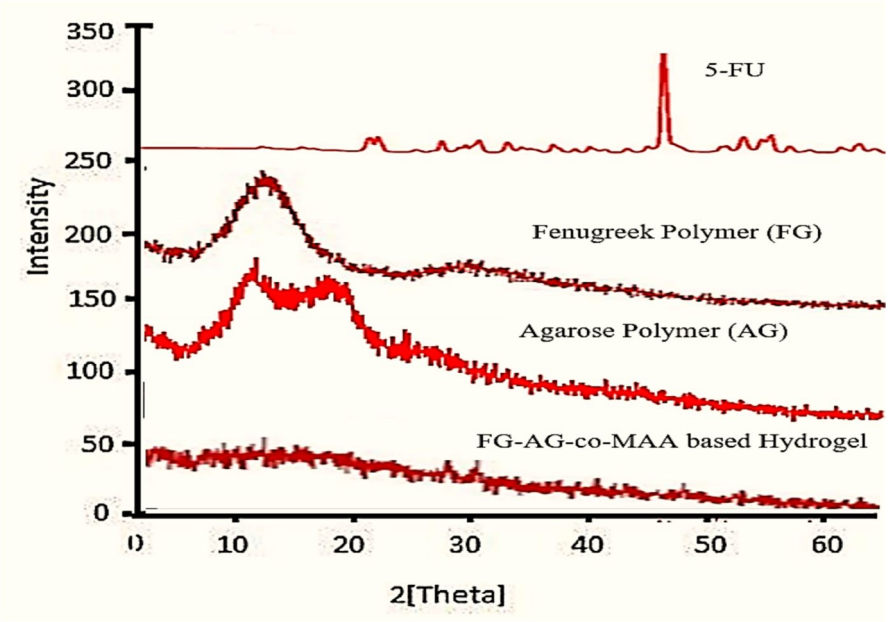

Fig. 12 XRD of 5-FU, fenugreek (FG), agarose (AG) and drug loaded nexus

conducted, and scanning was done between 11 and 79° at a rate of 55 degree/ min. The recorded diffractogram of Fenugreek is shown in Fig. 12. It is evident from the diffractogram that fenugreek has an intense peak within the region of 10.50–20.11° due to the presence of hydroxyl groups within its structure. These peaks indicate the crystalline nature of the fenugreek polymer. These findings are also evident from the research work of Pathak et al. (2014 while studying the physicochemical characterization and evaluation of anionic polymer-based nanoparticulated systems [31]. It was evident from the diffractogram that agarose has significant peaks at $2\theta = 14.11$o, 19.85o, and 27.17o. Peak near 19.34o was comparatively more intense. The prevalence of such peaks has also confirmed the semi-crystalline nature of agarose. Yan et al., 2020, developed a chitosan/agarose porous composite hydrogel and observed similar peaks with minor variations [18]. However, the drug and polymer peaks disappear in the final formulation (F9), whose XRD depicts dump, diffused peaks that confirm the amorphous nature and the molecular dispersal of the drug in the polymer matrix. A similar fact was observed by Ijaz et al., 2022 [8].

Energy-dispersive X-ray Spectrum (EDX) spectroscopy

EDX was performed to find out the elemental composition of 5-FU (fluorouracil), unloaded hydrogels, and 5-FU-loaded hydrogels. The results of EDX are summarized in Fig. 13. However, the EDX spectrum displays not only the existence of an element but also the weight of every element in a compound. Figure 13 shows that the EDX spectra of 5-FU contain carbon (39.60%), oxygen (24.82%), fluorine

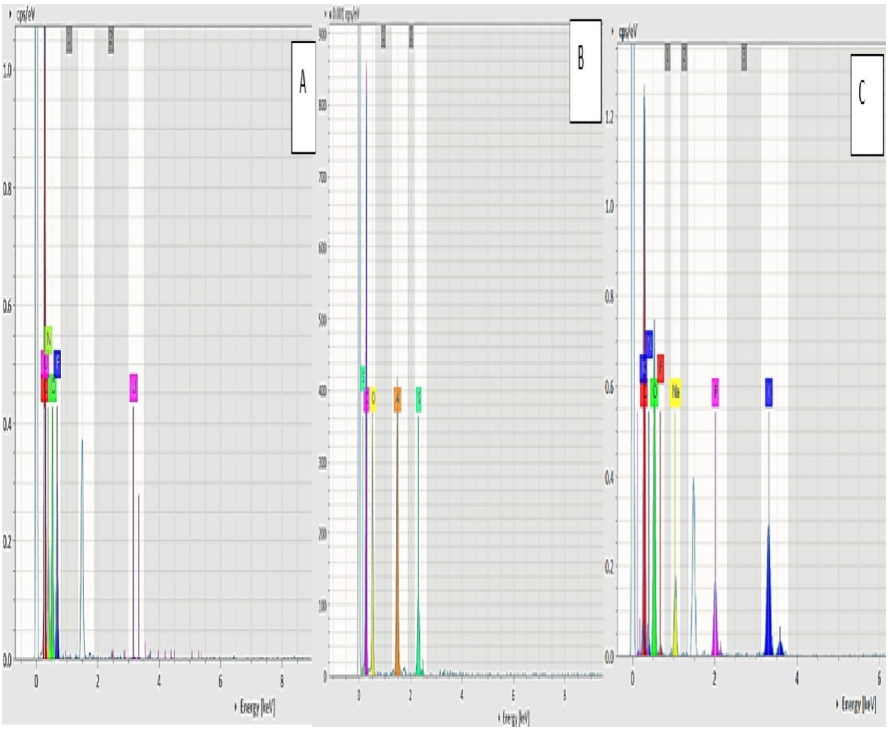

Fig. 13 EDX spectrum of 5-FU (5-fluorouracil) (**A**), EDX spectrum of unloaded hydrogel (**B**), EDX spectrum of 5-FU loaded hydrogel (**C**)

(13.98%), uranium (0.29%), and nitrogen (21.30%), respectively. Similar elements were reported by Yusefi et al. (2021) while working on 5-FU-loaded magnetic cellulose nanocomposites for treating colorectal cancer [32]. The unloaded nexus shows the presence of carbon, sulfur, and aluminum. However, the drug-loading nexus showed all elements of the drug as well as the unloaded nexus, which indicates efficient entrapment of the drug within the nexus. Mahmood et al. (2023) also reported changes in peaks of carbon and oxygen in the drug-loaded hydrogel, and the prominent appearance of peaks depicts successful grafting as well as drug loading into the polymeric network [19].

Scanning *electron* microscopy

Surface topological and morphological features of developed polymeric systems were evaluated via SEM, as shown in Fig. 14. SEM micrographs were recorded for optimized formulation (F9), demonstrating a heterogeneous framework with micro and macro pores consisting of interlinked polymeric chains. Moreover, SEM micrographs also depicted cracked, rough, wavy, irregular, interconnected, tangled, porous

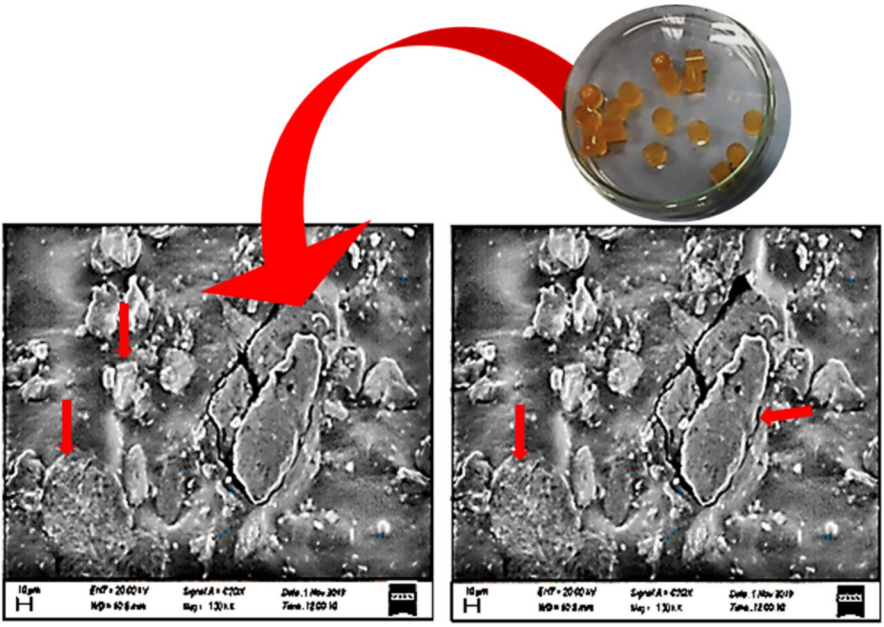

Fig. 14 SEM micrographs of prepared hydrogels

interstitial channels that facilitate the diffusion of physiological fluids, resulting in augmented swelling and drug release. Kim & Chu (2000) synthesized the dextran-methacrylate nexus and reported analogous findings [33]. Mukhopadhyay et al. (2014) formulated a pH-dependent N-succinyl chitosan-grafted polyacrylamide nexus and showed a rough, porous, and irregular nature of the nexus [34].

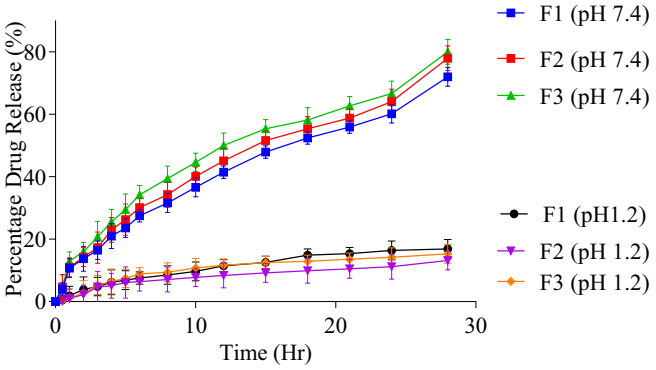

Fig. 15 Influence of Fenugreek concentration on 5-FU release (%)

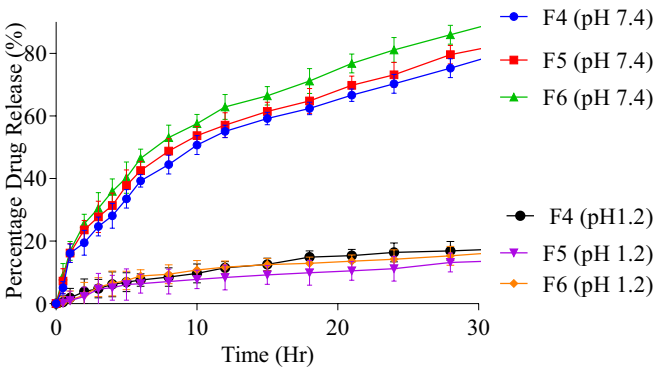

Fig. 16 Influence of Agarose concentration on 5-FU release (%)

In vitro release of 5-FU (fluorouracil) from fenugreek-agarose-based hydrogels

Drug release from dehydrated hydrogel implicates successive events like swelling-induced permeability, imbibition of media into the polymeric nexus, dissolution, and release of an entrapped moiety. The osmotic pressure gradient allows surrounding media to penetrate the polymeric nexus; the hydrogel swells in response to the diffusion of water; and interconnected channels allow drug release. In formulation, the F1-F3 effect of fenugreek on the percentage release of 5-FU was studied. The results are shown in Fig. 15. By increasing the amount of fenugreek (0.3–0.9 g), there was a significant increase in the percentage release of 5-FU because it relates to the swelling of hydrogels. Batool et al. (2021) synthesized and evaluated a 5-FU-loaded fenugreek base nexus and observed a similar fact. In formulations F4-F6, the influence of agarose on drug release showed an increment in the percentage release of 5FU, as shown in Fig. 16. By increasing the agarose concentration (1–2 g), drug release was increased (78–86%) in an alkaline solution (pH 7.4). On the other hand, at pH 1.2, the cumulative release was 6–6.4%. Drug release was increased by increasing

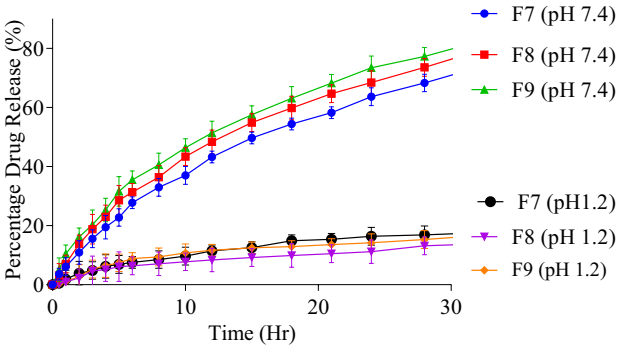

Fig. 17 Influence of MAA concentration on 5-FU release (%)

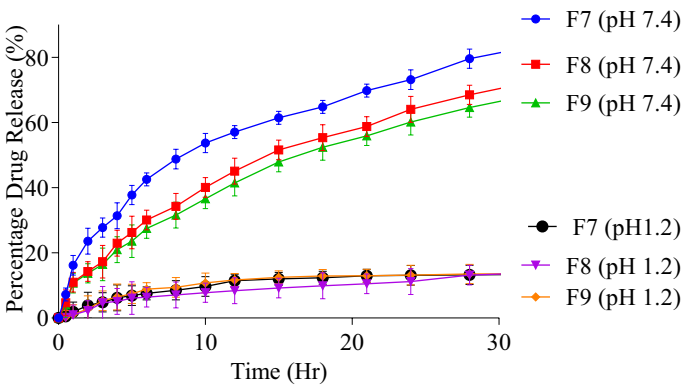

Fig. 18 Influence of MBA concentration on 5-FU release (%)

the concentration of agarose because of the presence of water-loving groups such as hydroxyl and carbonyl groups. These groups will bind with the hydroxyl group of water, so they increased the diffusion of 5-FU into the dissolution medium. These results are also evident from the previous research work of Nihat and her co-workers, who formulated a cytarabine-loaded nexus [14]. By increasing the concentration of monomer (MAA) from 20 to 30 g, cumulative drug release was increased from 80 to 88% at pH 7.4 and from 6.5% to 6.9% at pH 1.2, as shown in Fig. 17. As MAA concentration increased in formulations F7 to F9, cumulative drug release increased because methacrylic acid contains carboxylic acid groups, which become protonated, due to which there was the least drug release

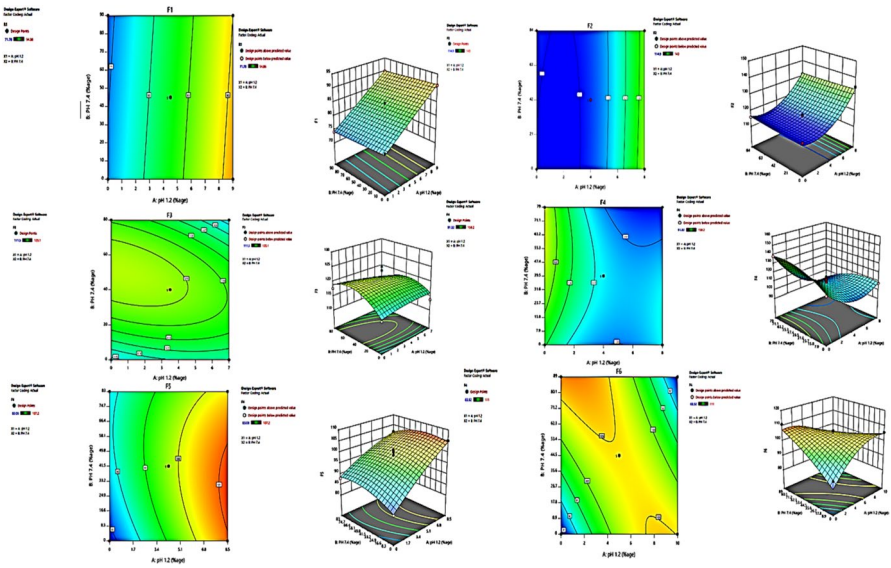

Fig. 19 RSM graph and contour plot from formulation (F1 to F6)

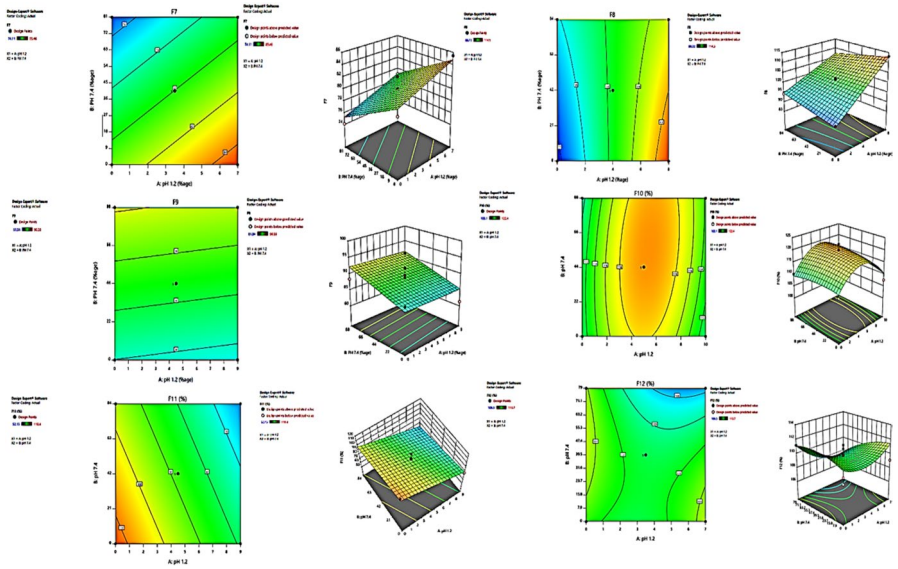

Fig. 20 RSM graph and contour plot from formulation (F7 to F12)

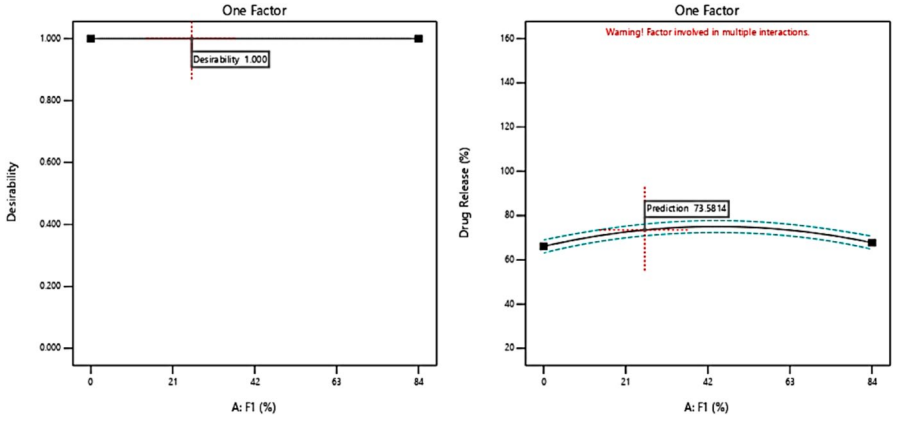

Fig. 21 Desirable and predicted drug release from formulation F1 to F12

at an acidic pH. Significant drug release was observed at 7.4 pH because, at this pH, carboxylic acid groups in methacrylic acid were converted into carboxylic anions, which led to the opening of polymeric channels. Moreover, the literature survey also reports the fact that electrostatic repulsive forces lead to the opening of the channel through which drug release occurs. Similar results were reported by Ijaz et al. (2021) while formulating a PE-loaded AX-co-MAA-based nexus [21]. The effect of increasing the concentration (0.25–0.75 g) of MBA on drug release (89.3–79.7%) is shown in Fig. 18. In formulation, the F10-F12 5-FU

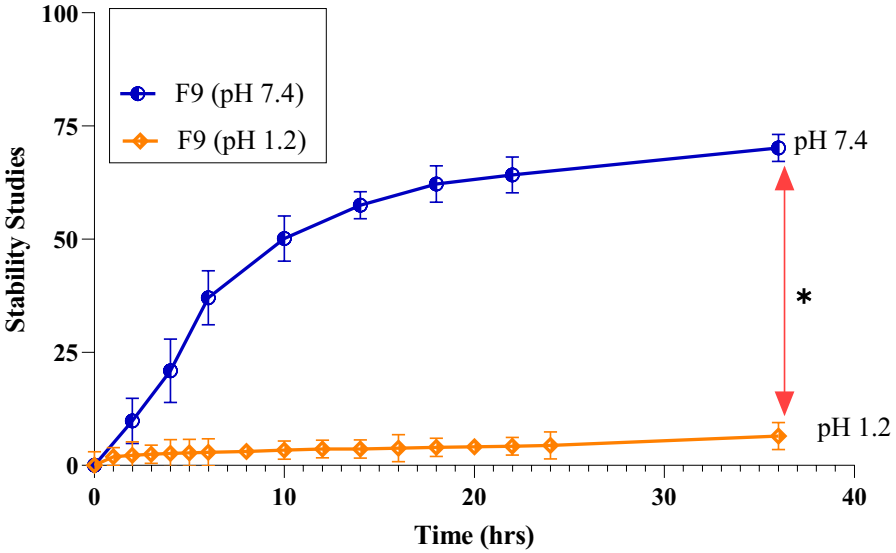

Fig. 22 Stability studies of F9 (Optimized formulation)

release percentage decreased (89–79%) because it depends on swelling and drug loading on hydrogels. A reduction in swelling is attributed to cross-linking density. While an increase in the number of crosslinkers causes a reduction in the free spaces present in polymeric networks, a dense and rigid structure is formed in which water or buffer solution cannot penetrate, which influences the drug release from hydrogels. Malik et al. (2020) prepared xanthan gum/chitosan-based hydrogels as a potential carrier for acyclovir and depicted that as the concentration of MBA increased in formulations F3 and F4, a decrease in acyclovir release (91.02–83.97%) was observed [20]. Similar findings were observed in our results. RSM and contour plots are shown in Figs. 19 and 20. Desirability and predicted drug release from formulations F1 to F12 are shown in Fig. 21.

Stability Studies

The effectiveness of the optimized batch was checked via stability studies, which were carried out as per ICH guidelines. The influence of relative humidity and temperature was checked. Stability studies showed that all formulations remain stable for up to 6 months (Fig. 22).

Evaluation of 5-FU (fluorouracil) release data through kinetic modeling

Release data of (F1–F12) formulations obtained via the DD solver was subjected to kinetic modeling. Different models, like zero order, first order, the Higuchi model, and the Korsmeyer Peppas model, were applied to get the value of R2 of all prepared formulations, as shown in Table 3. From the obtained results, it was clear that

Table 3 Kinetic modeling of data release

Formulation code	Zero order	First order	Higuchi model	Korsmeyer peppas	
Parameters	R^2	R^2	R^2	R^2	n value
F1	0.9044	0.7338	0.9737	0.9711	0.374
F2	0.9092	0.7439	0.9763	0.9783	0.352
F3	0.9021	0.7127	0.9728	0.9784	0.324
F4	0.9489	0.7293	0.9805	0.9603	0.535
F5	0.9488	0.7124	0.9805	0.9573	0.586
F6	0.9501	0.7354	0.9818	0.9537	0.645
F7	0.9025	0.6773	0.9732	0.9762	0.339
F8	0.9021	0.6480	0.9730	0.9804	0.311
F9 (Best Formulation)	0.9005	0.6315	0.9716	0.9812	0.288
F10	0.9753	0.6634	0.9988	0.9912	0.355
F11	0.9760	0.7279	0.9987	0.9932	0.389
F12	0.9742	0.7969	0.9984	0.9955	0.426

Table 4 Clinical observations of both controlled and treated rabbits (Treated with formulation F9)

Observations	Group (I) controlled	Group (II) treated
Sign of illness	Nil	Nil
Weight (kg) **Day 1 Day 7 Day 14**	2.08 2.05 2.08 2.07	2.08 2.05 2.08 2.07
Water intake **Day 1 Day 7 Day 14**	150 130 135	140 130 120
Food (g) **Day 1 Day 7 Day 14**	70 65 60	70 65 60
Dermal toxicity	Nil	Nil
Ocular toxicity	Nil	Nil
Mortality	Nil	Nil

formulation F9 followed the Higuchi model, i.e., drug release at a constant rate. The value of n is 0.288, which shows drug release occurs via fickian diffusion. Data was analyzed statistically via ANOVA (one-way ANOVA), which shows $p = 0.034$ ($P \leq 0.05$), which showed a significant difference between formulations. The result was analyzed via similarity and difference factor, which showed F9 showed a close resemblance to F3 as the similarity factor (*f1*) is 8.56 and the difference factor (*f2*) is 75.65.

Toxicity Studies

For acute oral toxicity studies, different parameters were studied, like clinical findings, blood analysis, and biochemical and histopathological findings. Clinical manifestations show no appropriate changes or effects after food intake and no change in body weight. No signs of dermal or ocular toxicity or mortality were observed, as

Table 5 Hematological observations of controlled and treated rabbits (Treated with formulation F9)

Parameters	Controlled	Treated
Hb (10–15) g/dL	4.3	10.4
WBCs × 10^3/µL	1.5	1.7
RBCs × 10^6/µL	2.16	5.35
HCT (%)	12.0	31.2
MCV (fL)	55.6	58.3
MCH pg/cell	19.9	19.4
MCHC g/dL	35.8	33.3
Platelets × 10^3/µL	42	106
Lymphocytes (%)	63.1	55.3
Neutrophils (%)	49	33.1

Table 6 Biochemical investigations of both control and treated rabbits (Treated with formulation F9)

Biochemical analysis	Group (I) control	Group (II) treated
ALT (IU/I)	54	84
AST (IU/I)	125	217
Uric acid (mg/dl)	0.1	0.5
ALP (IU/I)	30	43
UREA mmol/L	5.21	105
ALB (IU/I)	106	4.97
BUN (mg /dL)	50	49

shown in Table 4. Mahmood et al. (2023) formulated a diloxanide furoate-loaded intelligent nexus and reported similar facts [19]. Hematological studies give information about the pathological and physical state of animals. This study includes the results of both the control group (untreated) and the tested group (treated with drug-loaded hydrogel). Results were evaluated in terms of CBC (complete blood count), Hb (hemoglobin rate), WBCs (white blood cell count), RBCs (red blood cell count), HCT, MVC, MCH, MCHC, platelets, neutrophils, and lymphocytes in both controlled and treated groups. Results are given in Table 5. Values were within the normal range; no clinical toxicity was observed. Hb for the controlled group is 4.3, and for the treated group, it is 10.4 g/dL. WBCs for the controlled group are 1.5 × 103 and for the treated group are 1.7 × 103 /µL. HCT is 12% for the controlled group and 31.2% for the treated group. Platelets for the controlled group are 41 × 103/L, and for the treated group, they are 106 × 103/L. Lymphocytes are 63.1% in the control group and 55.3% in the treated group. Our results are in line with previous research studies [19]. Biochemical findings were given so that to investigate any toxic effects, RFTs (renal function tests) in which amounts of urea, uric acid, and creatinine were observed, LFTs (liver function tests) in which ALT and AST were observed, and metabolic biomarkers in which cholesterol and triglyceride were included were

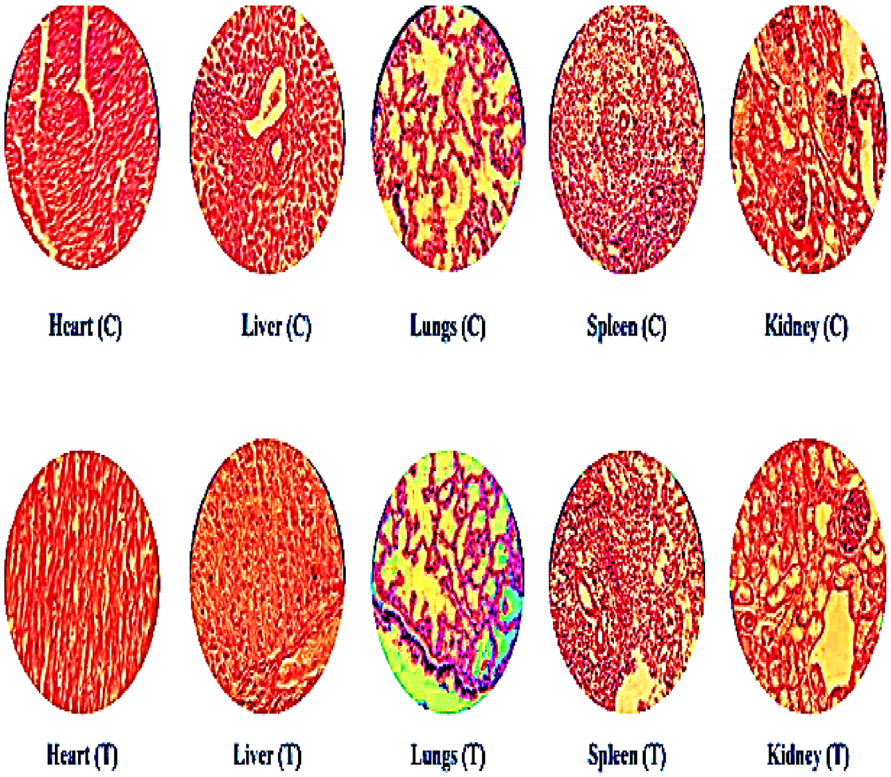

Fig. 23 Histopathological slides of the vital organs

also observed. Shown in Table 6. ALT for the controlled group is 54 (IU/L), and for the treated group, it is 84 (IU/L). AST for the controlled group is 125 (IU/L), and AST for the treated group is 217 (IU/L). Uric acid for the controlled group is 0.1 mg/dl, and for the treated group, it is 0.5 mg/dL**.** Shabir et al. (2022) performed a biochemical analysis of a black seed-based polysaccharide-grafted acrylic acid copolymer for oral delivery of insulin and reported that there is no significant difference in biochemical parameters between the controlled and treated groups [13]. In histopathological studies or investigations, any damage to vital organs and change in weight of tested rabbits were observed and compared with controlled rabbit organs. Vital organs include the brain, heart, liver, kidney, small intestine, and spleen. Part I was marked for controlled rabbits, and Part II was for tested rabbits. Results revealed that there was no toxic effect from loaded hydrogels. There was no change in organ attributes, as shown in Fig. 23 and Table 7. Malatani et al. (2023) formulated pH-sensitive mucin/chitosan-based Tofacitinib-loaded hydrogel microparticles and reported the fact that formulated hydrogels undergo no significant damage to vital organ-treated groups [35] (Table 8).

Table 7 Histopathological findings related to vital organs

Sr. No	Tissue	Comment
1	Heart (control)	Normal cardiomyocytes, no hypertrophy. Normal presence of collagenous material
2	Liver (control)	Evidence of liver damage characterized by bridging fibrosis (10%), many hepatocytes have double nuclei. High mitotic activity (hyperplasia is observed) around the blood vessels in the hepatic triad
3	Lung (control)	Clear alveoli, no fibrosis, no cumulation of inflammatory cells
4	Spleen (control)	Normal
5	Kidney (control)	No sign of nephritis or tubular disease
6	Liver (Treated)	Some necrotic areas are present, extensive collagen deposition around the portal triads. Bridging fibrosis is evident in the liver tissue
7	Heart (Treated)	Normal cardiomyocytes. Intact bl vessels. Normal heart
8	Kidney (Treated)	Normal glomeruli with filtered plasma and eosinic fluid. No sign of tubular necrosis or disease
9	Spleen (Treated)	Normal
10	Lungs (Treated)	Clear alveoli, no fibrosis, no cumulation of inflammatory cells

Table 8 Comparison between current and previous research

Sr No	Research	Reference
1	Bio-compatible, thermally stable and colonically degradable pectin-grafted-poly methacrylic acid nexus was formulated for delivery of 5-fuorouracil (5-FU) by employing Ethylene glycol dimethacrylate (EGDMA) as crosslinker. Methacrylic acid (MAA) serve as pH sensitive crosslinker. After 12 h, 90% drug release in pH 7.4	Minhas et al. [36]
2	Pectin-HPMC-co-AA based hydrogel was formulated for controlled delivery of Galantamine hydrobromide. HPMC and pactin was employed as polymer, acrylic acid as monomer and MBA as crosslinker. In pH 7.4 drug release was 75.36 to 87.62%	Bashir et al. [37]
3	pH responsive metformin loaded nexus was developed for sustained drug delivery. Acrylic acid and pectin loaded nexus was formulated by employing ethylene glycol dimethacrylate (EGDMA) as crosslinker. Formulated nexus showed 95.45% inpH 7.4 and 8.65% drug release in pH 1.2	Ali et al. [38]
4	Modified pectin grafted acrylic acid based nexus was formulated and drug release occur up to three days	Firyal and Hameed [39]
5	In current research work, 5-fluorouracil (5-FU) loaded fenugreek (FG), agarose (AG) and methacrylic acid (MAA) base hydrogel was formulated by employing N', N'methylene bisacrylamide (MBA) as a crosslinker. F9 showed significant swelling, drug loading as well as release. Formulated nexus F9 serve as promising nexus for delivery of 5-FU	Current Research work

Conclusions

pH-sensitive, controlled-release fenugreek and agarose-based hydrogels were prepared by free radical polymerization. The reaction was initiated by ammonium persulfate, and MBA was used as a cross-linker and MAA as a monomer. Swelling studies suggested their implication as a smart pH-sensitive drug delivery carrier as they showed high swelling percentages, drug loading, and subsequent release at a higher pH, i.e., 7.4. Fabricated hydrogels depict pH-dependent swelling and release for controlled delivery of 5-FU. Swelling and release kinetics were dependent on the amount of fenugreek, agarose, MAA, and MBA in fabricated hydrogels. By enhancing MAA, it was observed that swelling and release percentages were increased. Based on swelling and release data, F9 was selected as the optimized formulation. Mechanical strength studies revealed that hydrogels were of high tensile strength and capable of holding environmental stress. 5-FU loading into hydrogels was proven by EDX studies. The toxicity evaluation confirmed that the prepared hydrogel network was safe and non-toxic to living tissues. As fabricated hydrogels appear to be smart, they can therefore be employed for controlled delivery of 5-FU wherever pH-dependent delivery is required.

Supplementary Information The online version contains supplementary material available at https://doi.org/10.1007/s00289-024-05477-6.

Author contributions MM helped in writing paper. AM and RMS helped in designing the project. RA and FG conducted the study. HI and SA helped in refining the manuscript. BH and Z draw graphs.

Declarations

Conflict of interest The authors declare no competing interests.

References

1. Ajalli N, Pourmadadi M, Yazdian F, Rashedi H, Navaei-Nigjeh M, Díez-Pascual AM (2022) Chitosan/gamma-alumina/Fe3O4@ 5-FU nanostructures as promising nanocarriers: physiochemical characterization and toxicity activity. Molecules 27(17):5369
2. Very N, Hardivillé S, Decourcelle A, Thévenet J, Djouina M, Page A, Yazidi-Belkoura E (2022) Thymidylate synthase O-GlcNAcylation: a molecular mechanism of 5-FU sensitization in colorectal cancer. Oncogene 41(5):745–756
3. Chan WL, Choi CW, Wong IYH, Tsang THT, Lam ATC, Tse RPY, Law S (2022) Docetaxel, cisplatin, and 5-FU triplet therapy as conversion therapy for locoregionally advanced unresectable esophageal squamous cell carcinoma. Annals of Surg Oncology. 30:1–10
4. Zheng Y, Wang W, Zhao J, Wu C, Ye C, Huang M, Wang S (2019) Preparation of injectable temperature-sensitive chitosan-based hydrogel for combined hyperthermia and chemotherapy of colon cancer. Carbohyd Polym 222:115039
5. Ghobashy MM, Elbarbary AM, Hegazy DE (2021) Gamma radiation synthesis of a novel amphiphilic terpolymer hydrogel pH-responsive based chitosan for colon cancer drug delivery. Carbohyd Polym 263:117975
6. Shanmugapriya K, Kim H, Kang HW (2020) Epidermal growth factor receptor conjugated fucoidan/alginates loaded hydrogel for activating EGFR/AKT signaling pathways in colon cancer cells during targeted photodynamic therapy. Int J Biol Macromol 158:1163–1174
7. Martin BC, Minner EJ, Wiseman SL, Klank RL, Gilbert RJ (2008) Agarose and methylcellulose hydrogel blends for nerve regeneration applications. J Neural Eng 5(2):221

8. Guo J, Zhang R, Zhang L, Cao X (2018) 4D printing of robust hydrogels consisted of agarose nanofibers and polyacrylamide. ACS Macro Lett 7(4):442–446
9. de Araujo CMB, Ghislandi MG, Rios AG, da Costa GRB, do Nascimento BF, Ferreira AFP, Rodrigues AE (2022) Wastewater treatment using recyclable agar-graphene oxide biocomposite hydrogel in batch and fixed-bed adsorption column: Bench experiments and modeling for the selective removal of organics. Colloids Surf, A 639:128357
10. Liu C, Ning R, Lei F, Li P, Wang K, Jiang J (2022) Study on the structure and physicochemical properties of fenugreek galactomannan modified via octenyl succinic anhydride. Int J Biol Macromol 214:91–99
11. Ijaz H, Tulain UR, Minhas MU, Mahmood A, Sarfraz RM, Erum A, Danish Z (2022) Design and in vitro evaluation of pH-sensitive crosslinked chitosan-grafted acrylic acid copolymer (CS-co-AA) for targeted drug delivery. Int J Polym Mater Polym Biomater 71(5):336–348
12. Zafar N, Akhlaq M, Mahmood A, Ijaz H, Sarfraz RM, Hussain Z, Masood Z (2022) Facile synthesis and in vitro evaluation of semi-interpenetrating polymeric network. Polym Bull 80:1–29
13. Danish Z, Ijaz H, Razzaque G, Haq NU, Aslam MM (2022) Facile synthesis of three-dimensional porous hydrogel and its evaluation. Polym Bull 79(9):7407–7428
14. Batool N, Mahmood A, Sarfraz RM, Ijaz H, Zafar N, Hussain Z (2021) Formulation and evaluation of interpenetrating polymeric network for controlled drug delivery. Drug Dev Ind Pharm 47(6):931–946
15. Ijaz H, Tulain UR, Qureshi J (2018) Formulation and in vitro evaluation of pH-sensitive cross-linked xanthan gum-grafted acrylic acid copolymer for controlled delivery of perindopril erbumine (PE). Polym-Plast Technol Eng 57(5):459–470
16. Ijaz H, Tulain UR (2019) Development of interpenetrating polymeric network for controlled drug delivery and its evaluation. Int J Polym Mater Polym Biomater 68(18):1099–1107
17. Cheikh D, Majdoub H, Darder M (2022) An overview of clay-polymer nanocomposites containing bioactive compounds for food packaging applications. Appl Clay Sci 216:106335
18. Yan K, Xu F, Li S, Li Y, Chen Y, Wang D (2020) Ice-templating of chitosan/agarose porous composite hydrogel with adjustable water-sensitive shape memory property and multi-staged degradation performance. Colloids Surf, B 190:110907
19. Mahmood A, Mahmood A, Sarfraz RM, Ijaz H, Zafar N, Ashraf MU (2022) Hydrogel-based intelligent delivery system for controlled release of diloxanide furoate. Polym Bull 80:1–37
20. Malik NS, Ahmad M, Minhas MU, Tulain R, Barkat K, Khalid I, Khalid Q (2020) Chitosan/xanthan gum based hydrogels as potential carrier for an antiviral drug: fabrication, characterization, and safety evaluation. Front Chem 8:50
21. Azam F, Ijaz H, Qureshi J (2021) Functionalized crosslinked interpenetrating polymeric network for pH responsive colonic drug delivery. Int J Polym Mater Polym Biomater 70(9):646–655
22. Hu Y, Kim Y, Hong I, Kim M, Jung S (2021) Fabrication of flexible pH-responsive agarose/succinoglycan hydrogels for controlled drug release. Polymers 13(13):2049
23. Rana J, Goindi G, Kaur N, Sahu O (2022) Optimization and synthesis of cellulose acetate based grafted gel and study of swelling characteristics. Mater Today: Proc 48:1614–1619
24. Rahmani P, Shojaei A (2022) Developing tough terpolymer hydrogel with outstanding swelling ability by hydrophobic association cross-linking. Polymer 254:125037. https://doi.org/10.1016/j.polymer.2022.125037
25. Du X, Peng Y, Zhao C, Xing J (2022) Temperature/pH-responsive carmofur-loaded nanogels rapidly prepared via one-pot laser-induced emulsion polymerization. Colloids Surf, B 217:112611
26. Tang Z, Chen F, Chen Q, Zhu L, Yan X, Chen H, Zheng J (2017) The energy dissipation and Mullins effect of tough polymer/graphene oxide hybrid nanocomposite hydrogels. Polym Chem 8(32):4659–4672. https://doi.org/10.1039/C7PY01068K
27. Abdullah O, Usman Minhas M, Ahmad M, Ahmad S, Barkat K, Ahmad A (2018) Synthesis, optimization, and evaluation of polyvinyl alcohol-based hydrogels as controlled combinatorial drug delivery system for colon cancer. Adv Polym Technol 37(8):3348–3363
28. El-Bahy GMS (2005) FTIR and Raman spectroscopic study of Fenugreek (Trigonella foenum graecum L.) seeds. J Appl Spectrosc 72(1):111–116. https://doi.org/10.1007/s10812-005-0040-6
29. Rotjanasuworapong K, Thummarungsan N, Lerdwijitjarud W, Sirivat A (2020) Facile formation of agarose hydrogel and electromechanical responses as electro-responsive hydrogel materials in actuator applications. Carbohyd Polym 247:116709
30. Pal P, Pandey JP, Sen G (2018) Sesbania gum based hydrogel as platform for sustained drug delivery: An 'in vitro'study of 5-Fu release. Int J Biol Macromol 113:1116–1124

31. Pathak D, Kumar P, Kuppusamy G, Gupta A, Kamble B, Wadhwani A (2014) Physicochemical characterization and toxicological evaluation of plant-based anionic polymers and their nanoparticulated system for ocular delivery. Nanotoxicology 8(8):843–855
32. Yusefi M, Lee-Kiun MS, Shameli K, Teow SY, Ali RR, Siew KK, Kuča K (2021) 5-Fluorouracil loaded magnetic cellulose bionanocomposites for potential colorectal cancer treatment. Carbohydr Polym 273:118523
33. Kim SH, Chu CC (2000) Synthesis and characterization of dextran–methacrylate hydrogels and structural study by SEM. J Biomed Mater Res: An Off J Soc Biomater Jpn Soc Biomater 49(4):517–527
34. Mukhopadhyay P, Sarkar K, Bhattacharya S, Bhattacharyya A, Mishra R, Kundu PP (2014) pH sensitive N-succinyl chitosan grafted polyacrylamide hydrogel for oral insulin delivery. Carbohyd Polym 112:627–637
35. Ijaz H, Tulain UR, Azam F, Qureshi J (2019) Thiolation of arabinoxylan and its application in the fabrication of pH-sensitive thiolated arabinoxylan grafted acrylic acid copolymer. Drug Dev Ind Pharm 45(5):754–766
36. Minhas MU, Ahmad M, Anwar J, Khan S (2018) Synthesis and characterization of biodegradable hydrogels for oral delivery of 5-fluorouracil targeted to colon: screening with preliminary in vivo studies. Adv Polym Technol 37(1):221–229
37. Bashir S, Zafar N, Lebaz N, Mahmood A, Elaissari A (2020) Hydroxypropyl methylcellulose-based hydrogel copolymeric for controlled delivery of galantamine hydrobromide in Dementia. Processes 8(11):1350
38. Ali L, Ahmad M, Aamir MN, Minhas MU, Shah HH, Shah MA (2020) Cross-linked pH-sensitive pectin and acrylic acid based hydrogels for controlled delivery of metformin. Pak J Pharm Sci 33(4):1483–1491
39. Firyal MA, Hameed MA (2018) Controlled drug release of grafted pectin. J Drug Deliv Ther 8(5-s):215–222

Authors and Affiliations

Maria Malook[1] · Asif Mahmood[2] · Hira Ijaz[3] · Rai Muhammad Sarfraz[4] · Muhammad Rauf Akram[4] · Bilal Haroon[1,4] · Zulcaif Ahmad[5] · Sadaf Ayub[6] · Faisal Gulzar[7]

✉ Asif Mahmood
asif.mahmood@uoc.edu.pk

✉ Hira Ijaz
pharmacisthira@gmail.com

[1] School of Pharmaceutical Sciences, Faculty of Pharmacy, The University of Lahore, Sargodha campus, Lahore, Pakistan

[2] Department of Pharmacy, University of Chakwal, Chakwal, Pakistan

[3] Department of Pharmaceutical Sciences, Pak-Austria Fachhochschule: Institute of Applied Sciences and Technology, Mang, Khanpur Road, Haripur 22620, Khyber Pakhtunkhwa, Pakistan

[4] Faculty of Pharmacy, University of Sargodha, Sargodha, Punjab, Pakistan

[5] Riphah Institute of Pharmaceutical Sciences, Riphah International University Lahore, Chamru Pur Lahore, Pakistan

[6] College of Nursing Chakwal, Chakwal, Pakistan

[7] Department of Pharmacy, The University of Chenab, Gujrat, Pakistan